System-size-dependent avalanche statistics in the limit of high disorder

Viktória Kádár and Ferenc Kun ⬡*

Department of Theoretical Physics, University of Debrecen, P.O. Box 5, H-4010 Debrecen, Hungary
and Institute for Nuclear Research, Hungarian Academy of Sciences (Atomki), P.O. Box 51, H-4001 Debrecen, Hungary

We investigate the effect of the amount of disorder on the statistics of breaking bursts during the quasistatic fracture of heterogeneous materials. We consider a fiber bundle model where the strength of single fibers is sampled from a power-law distribution over a finite range, so that the amount of materials' disorder can be controlled by varying the power-law exponent and the upper cutoff of fibers' strength. Analytical calculations and computer simulations, performed in the limit of equal load sharing, revealed that depending on the disorder parameters the mechanical response of the bundle is either perfectly brittle where the first fiber breaking triggers a catastrophic avalanche, or it is quasibrittle where macroscopic failure is preceded by a sequence of bursts. In the quasibrittle phase, the statistics of avalanche sizes is found to show a high degree of complexity. In particular, we demonstrate that the functional form of the size distribution of bursts depends on the system size: for large upper cutoffs of fibers' strength, in small systems the sequence of bursts has a high degree of stationarity characterized by a power-law size distribution with a universal exponent. However, for sufficiently large bundles the breaking process accelerates towards the critical point of failure, which gives rise to a crossover between two power laws. The transition between the two regimes occurs at a characteristic system size which depends on the disorder parameters.

I. INTRODUCTION

The disorder of materials plays a crucial role in fracture phenomena when subject to mechanical loads. Experiments and theoretical calculations revealed that under constant or slowly varying external loads the fracture of heterogeneous materials proceeds in bursts of local breakings [1–6]. Such crackling events can be recorded in the form of acoustic signals providing insight into the microscopic dynamics of the fracture process [7–10]. Cracking bursts can be considered as precursors of the ultimate failure of the system, so that they can be exploited to forecast the impending catastrophic event [10–18].

The intensity of the crackling activity has been found to depend on the degree of materials' disorder [11,19,20]: in the limiting case of zero disorder, the ultimate failure occurs in an abrupt way with hardly any precursory activity [21,22]. However, the presence of disorder gives rise to a gradual cracking process where macroscopic failure occurs as a result of the intermittent steps of damage accumulation [23–25]. Recently, experiments have been performed on the compressive failure of porous glass samples where the degree of heterogeneity could be well controlled during the sample preparation [11]. These experiments have shown that increasing disorder gives rise to a more intensive bursting activity with a higher number of cracking events whose size spans a broader range. As a consequence, the precision of failure forecast methods was found to improve with increasing disorder [11].

Motivated by these recent findings, here our goal is to investigate the statistics of crackling noise in the limiting case

of extremely high disorder. The fiber bundle model (FBM) provides an adequate framework [26–32] to study the statistics of breaking avalanches allowing for a simple way to control the degree of disorder [31,33–37]. In FBMs the sample is discretized in terms of parallel fibers where controlling the mechanical response, strength, and interaction of fibers various types of materials' behaviors can be captured. Disorder can be represented by the random strength of fibers while their Young modulus is kept constant. In our study, high disorder is realized by a power-law distribution of fibers' strength over a finite range where the amount of disorder can be controlled by the exponent and by the upper cutoff of the strength values.

Assuming equal load sharing after fiber breakings, we demonstrate that the fat-tailed microscale disorder has a substantial effect on the statistics of breaking bursts of fibers. In particular, we show that the functional form of the burst size distribution depends on the size of the bundle: when the upper cutoff of fibers' strength is infinite the burst size distribution is a power law with a universal exponent. However, in the case of finite upper cutoff strength, for small system sizes the size distribution is identical with the one of the infinite cutoff strength. Deviations start at a characteristic system size beyond which a crossover occurs to another functional form. We give an explanation of the system-size-dependent avalanche statistics in terms of the extreme order statistics of breaking thresholds.

II. FIBER BUNDLE MODEL WITH FAT-TAILED DISORDER

We consider a bundle of N parallel fibers, which are assumed to have a perfectly brittle behavior with a Young's modulus E and breaking threshold σ_{th}. The Young's modulus

---

*Corresponding author: ferenc.kun@science.unideb.hu

is assumed to be constant $E = 1$ so that materials' disorder is captured by the randomness of the breaking threshold σ_{th}. The strength of individual fibers σ_{th}^i, $i = 1, \ldots, N$ is sampled from a probability density $p(\sigma_{th})$. The amount of disorder in the system can be controlled by varying the range $\sigma_{th}^{\min} \leqslant \sigma_{th} \leqslant \sigma_{th}^{\max}$ of strength values and by the functional form of $p(\sigma_{th})$. FBMs with moderate amount of disorder have been widely studied in the literature considering uniform, Weibull, and Gaussian distributions making the avalanche statistics of this universality class well understood [28,32].

To realize the limiting case of extremely high disorder, a fat-tailed disorder distribution is considered; i.e., we implement a power-law distribution of breaking thresholds over the range $\sigma_{th}^{\min} \leqslant \sigma_{th} \leqslant \sigma_{th}^{\max}$ with the probability density

$$p(\sigma_{th}) = \begin{cases} 0, & \sigma_{th} < \sigma_{th}^{\min}, \\ A\sigma_{th}^{-(1+\mu)}, & \sigma_{th}^{\min} \leqslant \sigma_{th} \leqslant \sigma_{th}^{\max}, \\ 0, & \sigma_{th}^{\max} < \sigma_{th}. \end{cases} \quad (1)$$

In our calculations, the lower bound of thresholds $\sigma_{th}^{\min}$ is fixed to $\sigma_{th}^{\min} = 1$, while the amount of disorder is controlled by varying the power-law exponent μ and the upper bound $\sigma_{th}^{\max}$ of thresholds. The value of $\sigma_{th}^{\max}$ covers the range $\sigma_{th}^{\min} \leqslant \sigma_{th}^{\max} \leqslant +\infty$, while the disorder exponent is varied in the interval $0 \leqslant \mu < 1$. For this choice of μ, in the limiting case of an infinite upper bound $\sigma_{th}^{\max} \to \infty$ the thresholds do not have a finite average; hence, varying the two parameters μ and $\sigma_{th}^{\max}$ the amount of disorder can be tuned in the bundle between the extremes of zero and infinity. Of course, at finite cutoffs $\sigma_{th}^{\max}$, the average fiber strength $\langle \sigma_{th} \rangle$ is always finite; however, the specific values of $\sigma_{th}^{\max}$ and μ have a very strong effect on the behavior of the system both on the macro- and microscales. The cumulative distribution $P(\sigma_{th})$ can be obtained from the normalized density as

$$P(\sigma_{th}) = \begin{cases} 0 & \sigma_{th} < \sigma_{th}^{\min}, \\ \frac{\sigma_{th}^{-\mu} - (\sigma_{th}^{\min})^{-\mu}}{(\sigma_{th}^{\max})^{-\mu} - (\sigma_{th}^{\min})^{-\mu}}, & \sigma_{th}^{\min} \leqslant \sigma_{th} \leqslant \sigma_{th}^{\max}, \\ 1 & \sigma_{th}^{\max} < \sigma_{th}. \end{cases} \quad (2)$$

After fiber failure, we assume that the excess load of broken fibers is equally redistributed over the remaining intact ones. Hence, the constitutive equation $\sigma(\varepsilon)$ of the bundle can be obtained from the general form $\sigma(\varepsilon) = E\varepsilon[1 - P(E\varepsilon)]$ by substituting the distribution function $P(x)$ from Eq. (2)

$$\sigma(\varepsilon) = \begin{cases} \varepsilon, & 0 \leqslant \varepsilon \leqslant \varepsilon_{\min}, \\ \frac{\varepsilon(\varepsilon^{-\mu} - \varepsilon_{\max}^{-\mu})}{\varepsilon_{\min}^{-\mu} - \varepsilon_{\max}^{-\mu}}, & \varepsilon_{\min} \leqslant \varepsilon \leqslant \varepsilon_{\max}, \\ 0, & \varepsilon_{\max} < \varepsilon. \end{cases} \quad (3)$$

For brevity, we introduce the notation $\varepsilon_{\min} = \sigma_{th}^{\min}/E$, $\varepsilon_{\max} = \sigma_{th}^{\max}/E$, with $E = 1$, for the lower and upper bounds of strength in terms of strain. The stress-strain relation of the bundle is illustrated in Fig. 1. Perfectly linear behavior is obtained up to the lower bound $\varepsilon_{\min}$, since no fibers break in this regime. After fiber breaking sets on, the constitutive curve becomes gradually nonlinear and develops a maximum whose position ε_c and value σ_c define the tensile strength of the bundle. Both the critical strain ε_c and stress σ_c depend on
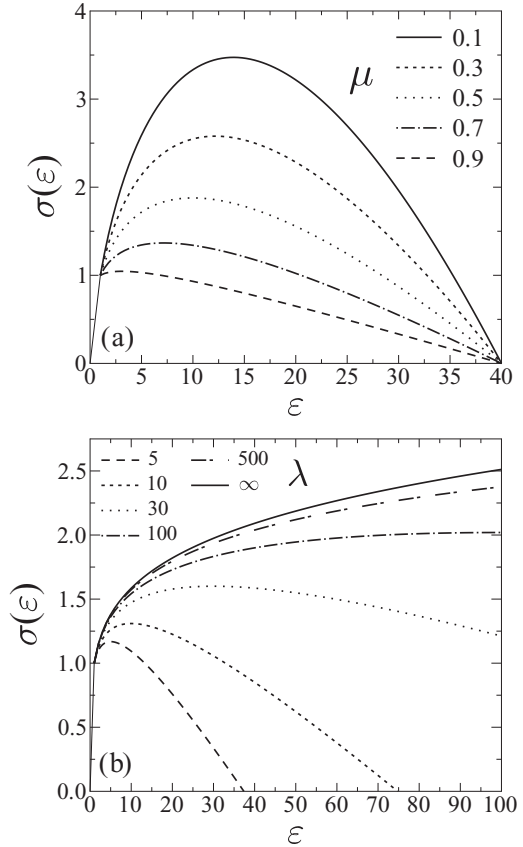

FIG. 1. Stress-strain curves $\sigma(\varepsilon)$ of the bundle (a) for a fixed value of the upper cutoff $\varepsilon_{\max} = 40$ varying the exponent μ, and (b) for a fixed $\mu = 0.7$ exponent varying the upper cutoff $\varepsilon_{\max}$ by means of the multiplication factor λ, where $\varepsilon_{\max} = \lambda \varepsilon_{\max}^c$. Approaching the phase boundary, in both cases the system becomes more and more brittle; i.e., the maximum of $\sigma(\varepsilon)$ is preceded by a smaller and smaller amount of fiber breakings. For comparison, the curve corresponding to the case of an infinite upper cutoff $\varepsilon_{\max} \to \infty$ is also presented.

the degree of disorder characterized by μ and $\varepsilon_{\max}$:

$$\varepsilon_c = \varepsilon_{\max}(1 - \mu)^{1/\mu} \quad (4)$$

and

$$\sigma_c = \frac{\mu(1 - \mu)^{1/\mu - 1}\varepsilon_{\max}^{1-\mu}}{\varepsilon_{\min}^{-\mu} - \varepsilon_{\max}^{-\mu}}. \quad (5)$$

Recently, we have shown that if the threshold distribution (1) of the model is sufficiently narrow, already the first fiber breaking can trigger the immediate failure of the entire bundle [38]. It can be observed in Fig. 1 that this occurs when the position of the maximum of the constitutive curve ε_c coincides with the lower bound $\varepsilon_{\min}$ of the fibers' strength. It follows that for all exponent values μ there exists a critical upper bound $\varepsilon_c^{\max}$ so that in the range $\varepsilon_{\max} < \varepsilon_{\max}^c$ the bundle exhibits a perfectly brittle behavior. Perfect brittleness means that under stress or strain controlled loading the breaking of the weakest fiber gives rise to an immediate abrupt failure of the bundle or in a softening behavior, respectively. The critical
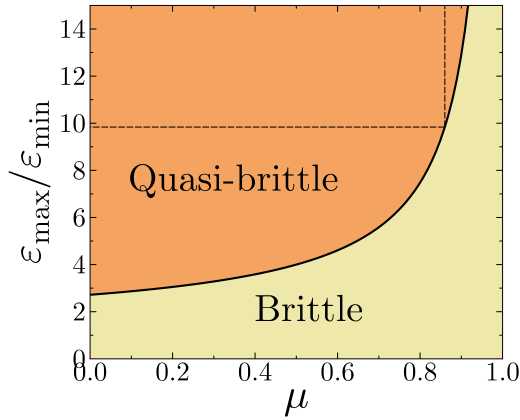
FIG. 2. Phase diagram of the system. The phase boundary separating the brittle and quasibrittle macroscopic response is given by Eq. (6). Under stress controlled loading, in the brittle phase the bundle suffers immediate abrupt failure at the breaking of the weakest fiber, while in the quasibrittle phase failure is preceded by a sequence of breaking bursts. For $\mu \geqslant 1$ the bundle is always in the brittle phase. The horizontal and vertical dashed lines indicate the parameter sets for which avalanche size distributions were determined by computer simulations.

upper bound can be obtained from Eqs. (4) and (5) as

$$\varepsilon_{\max}^{c} = \frac{\varepsilon_{\min}}{(1-\mu)^{1/\mu}}. \quad (6)$$

The results imply that at a given value of the exponent μ in the parameter regime $\varepsilon_{\max} > \varepsilon_{\max}^{c}$ a quasibrittle response is obtained where macroscopic failure is preceded by breaking avalanches. The phase boundary separating the brittle and quasibrittle behaviours of the system is given by the relation (6). The phase diagram of the system is illustrated in Fig. 2 on the μ-$\varepsilon_{\max}$ plane. Note that as the exponent μ approaches 1 from below the value of $\varepsilon_{\max}^{c}$ diverges so that the regime $\mu \geqslant 1$ is always brittle. When presenting results at a fixed exponent μ, it is instructive to characterize the upper cutoff $\varepsilon_{\max}$ of fibers strength relative to the corresponding point of the phase boundary $\varepsilon_{\max}^{c}(\mu)$. Hence, we introduce the parameter $\lambda = \varepsilon_{\max}/\varepsilon_{\max}^{c}$, which can take any value in the range $\lambda \geqslant 1$ (equality holds on the phase boundary between the brittle and quasibrittle phases).

Recently, we have demonstrated that the fat-tailed microscale disorder gives rise to an anomalous size scaling of the macroscopic strength of the bundle [38]. For finite upper cutoffs of fibers' strength $\varepsilon_{\max}$, the average strength of the bundle $\langle \varepsilon_c \rangle$ was found to increase with the number N of fibers as

$$\langle \varepsilon_c \rangle \sim N^{1/\mu}. \quad (7)$$

The usual decreasing behavior of strength [39,40] gets restored beyond a characteristic system size N_c, which depends on the disorder parameters as

$$N_c \sim \varepsilon_{\max}^{\mu}. \quad (8)$$

We could explain this interesting effect based on the extreme order statistics of the strength of single fibers; i.e., we pointed out that the bundle strength increases until the strongest
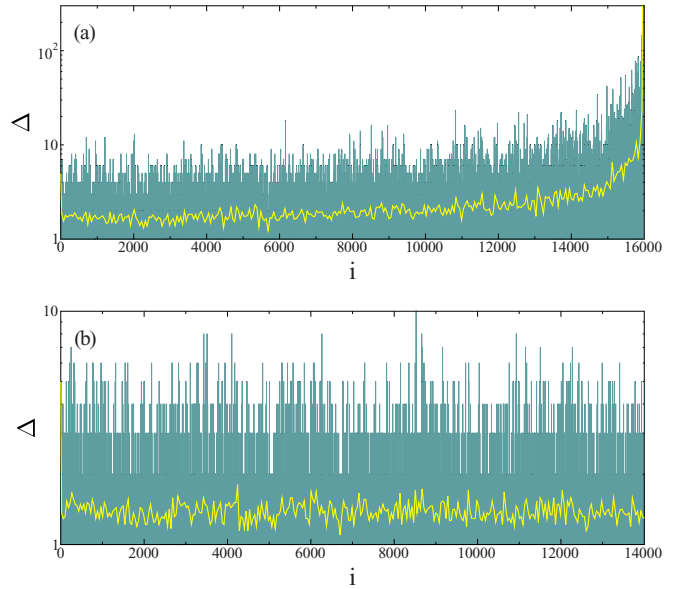

FIG. 3. Series of bursts in a small system of $N = 10^5$ fibers at the exponent $\mu = 0.8$ for two different values of the upper cutoff (a) $\lambda = 100$ and (b) $\lambda = +\infty$. The size of bursts Δ is presented as a function of the order number i of events. The yellow lines represent the moving average of burst sizes Δ averaging over 25 consecutive data points.

fiber dominates the ultimate failure of the system [38]. For sufficiently small systems, at high cutoffs $\varepsilon_{\max}$, the strongest fiber can be so strong that it can keep the entire load on the system. Beyond the characteristic system size N_c, this is no longer possible so that the average strength decreases with N. In the following we show that the fat-tailed disorder of fibers' strength gives rise also to a complex behavior of the statistics of breaking bursts when the parameters μ and $\varepsilon_{\max}$ are varied.

III. STATISTICS OF BREAKING BURSTS

Inside the quasibrittle phase, we analyze the fracture process of the bundle under quasistatic loading, which is realized by slowly increasing the external load to provoke the breaking of a single fiber at a time. For simplicity, we assume that the load of the broken fiber is equally redistributed over the intact ones, which may trigger additional breakings, followed again by load redistribution. As a consequence of the repeated breaking and load redistribution steps, an avalanche emerges which stops when all the remaining intact fibers are sufficiently strong to keep the elevated load. Global failure occurs in the form of a catastrophic avalanche which destroys the entire system. The size Δ of the avalanche is defined as the number of fibers breaking in the correlated trail.

A. Acceleration towards failure

Inside the brittle phase (see Fig. 2) the first avalanche already triggers the immediate catastrophic failure of the system. However, in the quasibrittle parameter regime the system gradually approaches failure through a sequence of bursts whose size Δ spans a broad range. Representative examples of the series of bursts are shown in Fig. 3 for two different values
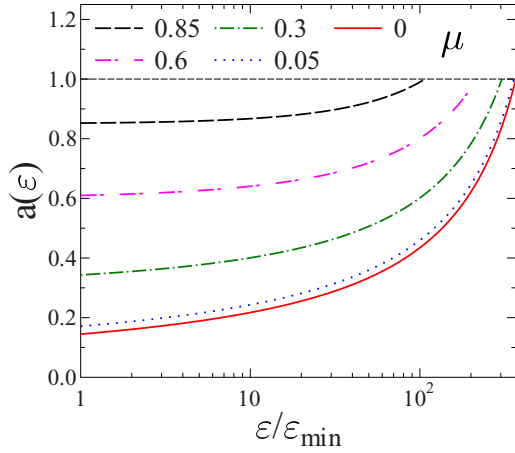
FIG. 4. The average number of breaking fibers $a(\varepsilon)$ (9) triggered by the failure of one fiber due to the increase of the external load for several values of the disorder exponent μ. The cutoff strength ε_{max} is fixed to $\varepsilon_{max}/\varepsilon_{min} = 1000$. All curves are presented from ε_{min} to the corresponding value of $\varepsilon_c(\mu, \varepsilon_{max})$. For $\mu \to 0$ the critical point converges to $\varepsilon_c = \varepsilon_{max}/e$.

of the upper cutoff $\lambda = 100$, $\lambda = +\infty$ at the same exponent $\mu = 0.8$. For the infinite cutoff in Fig. 3(b) the burst size Δ fluctuates; however, its moving average remains practically constant. It means that in spite of the increasing external load the system does not show any acceleration towards failure. In fact, in this case the constitutive curve of the bundle (see Fig. 1) does not have a maximum, it monotonically increases until the last fiber breaks the bundle. Contrary to this, for a finite upper cutoff in Fig. 3(a) the system approaches global failure through an increasing average size of bursts. At the critical point of failure a catastrophic avalanche emerges, while the catastrophic event is absent when the cutoff strength is infinite.

To understand the behavior of the burst sequence, it is instructive to calculate the average number a of fiber breakings triggered immediately by the failure of a single fiber at the strain ε [29,32]. The load $\sigma = E\varepsilon$ dropped by the broken fiber is equally shared by the intact ones of number $N[1 - P(\sigma)]$, giving rise to the stress increment $\Delta\sigma = \sigma/N[1 - P(\sigma)]$. Multiplying $\Delta\sigma$ with the probability density $p(E\varepsilon)$ of failure thresholds and with the total number of fibers N, the average number of triggered breakings a can be cast into the form

$$a(\varepsilon) = \frac{E\varepsilon p(E\varepsilon)}{1 - P(E\varepsilon)} = \frac{\mu}{1 - \left(\frac{\varepsilon}{\varepsilon_{max}}\right)^{\mu}}. \tag{9}$$

The right-hand side of the equation was obtained by substituting the PDF p (1) and the CDF P (2) of failure thresholds of our model. The expression has to be evaluated over the range $\varepsilon_{min} \leqslant \varepsilon \leqslant \varepsilon_c$ which is illustrated by Fig. 4 for several values of the exponent μ at a fixed upper cutoff $\varepsilon_{max} = 1000$. It can be seen that as the system approaches the critical point of global failure ε_c (4), the value of a increases to 1 indicating the acceleration of the failure process and the onset of the catastrophic avalanche at the critical point.

It follows from Eq. (9) that for an infinite upper cutoff $\varepsilon_{max} \to \infty$, the average number of triggered breakings a takes

a constant value $a = \mu < 1$, which implies stable cracking and a constant average burst size as could be inferred from Fig. 3(b). When the cutoff strength ε_{max} is finite, for sufficiently small strains ε the value of a still can be considered constant $a \approx \mu$ and the acceleration of the bursting process is constrained to the vicinity of the critical point ε_c. Equation (9) implies that the effect is more pronounced when $\varepsilon_c \ll \varepsilon_{max}$, which requires μ to be close to 1 and a large value of the cutoff strength according to Eq. (4). Figure 4 shows this behavior for $\mu = 0.85$, where a remains close to μ for a broad range of ε, while for smaller exponents μ a considerable acceleration is observed from the beginning of the failure process. In the limit $\mu \to 0$ the number of triggered breakings takes the form

$$a(\varepsilon) \approx \frac{1}{\ln(\varepsilon_{max}/\varepsilon)}, \tag{10}$$

while the critical point ε_c converges to $\varepsilon_c = \varepsilon_{max}/e$ (see also Fig. 4).

Note, however, that in the derivation of a implicitly an infinite system size is assumed. Later we show that to obtain acceleration towards failure and a catastrophic avalanche at finite cutoff strengths, the size of the system N has to exceed a characteristic value, which is a consequence of the fat-tailed disorder.

B. Size distribution of bursts

The statistics of breaking bursts can be characterized by the distribution $p(\Delta)$ of their size Δ. The complete size distribution $p(\Delta)$ can be obtained analytically by substituting $a(\varepsilon)$ into the generic form [29,32,41]

$$\frac{p(\Delta)}{N} = \frac{\Delta^{\Delta-1}e^{-\Delta}}{\Delta!} \int_0^{x_c} p(x)a(x)$$
$$\times [1 - a(x)]^{\Delta-1}e^{\Delta a(x)}dx, \tag{11}$$

where for the upper limit of integration x_c we have to insert the strength of the bundle. Utilizing the approximation $\Delta! \simeq \Delta^{\Delta}e^{-\Delta}\sqrt{2\pi\Delta}$, in the limiting case of an infinite upper cutoff with $a(\varepsilon) = \mu$ the burst size distribution can be cast into a simple analytic form

$$\frac{p(\Delta)}{N} \simeq \Delta^{-\tau}e^{-\Delta/\Delta^*}. \tag{12}$$

A power law of exponent $\tau = 3/2$ is obtained followed by an exponential cutoff. Here Δ^* denotes the characteristic burst size, which controls the cutoff of the distribution

$$\Delta^* = \frac{1}{\mu - 1 - \ln\mu}. \tag{13}$$

This result means that at an infinite upper cutoff of fiber strength $\varepsilon_{max} = +\infty$ the size distribution of bursts always follows a simple power law of a universal exponent $\tau = 3/2$, where the value of the disorder exponent μ controls only the cutoff burst size Δ^*. Using the Taylor expansion of logarithm around 1, it can easily be shown that as $\mu \to \mu_c = 1$ the cutoff burst size has a power-law divergence

$$\Delta^* \sim (\mu_c - \mu)^{-\nu}, \tag{14}$$

with a universal exponent $\nu = 2$. Burst size distributions obtained by computer simulations of a bundle of size $N = 10^6$
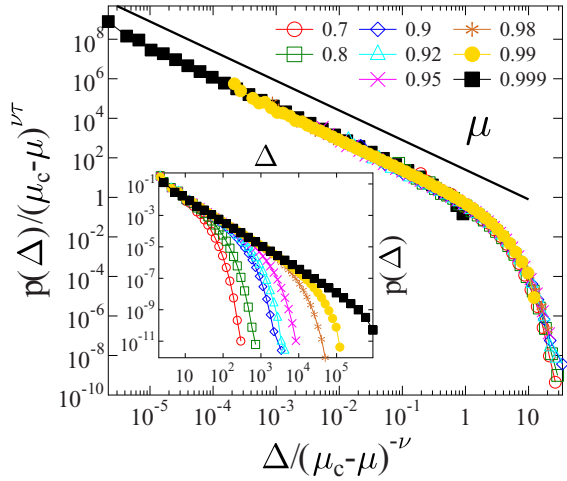
FIG. 5. Inset: Size distribution of bursts $p(\Delta)$ for a bundle of $N = 10^6$ fibers at several values of the disorder exponent μ when the cutoff strength of fibers is infinite $\varepsilon_{\max} = +\infty$. Main panel: Data collapse of the curves of the inset obtained by rescaling with a power of the distance from the critical point $\mu_c = 1$. Along the horizontal axis the scaling exponent is $\nu = 2$ in agreement with Eq. (14), while along the vertical axis the product $\nu\tau$ is used with $\tau = 3/2$. The straight line represents a power law of exponent $3/2$.

fibers are presented in the inset of Fig. 5 for several μ values using an infinite cutoff strength. An excellent agreement is obtained with the analytical predictions. The main panel of Fig. 5 demonstrates that rescaling the distributions with $(\mu_c - \mu)^{-\nu}$ the curves of different μ can be collapsed on the top of each other, which confirms the validity of the scaling law (14). In Ref. [42] we also showed that approaching $\mu_c = 1$ at $\varepsilon_{\max} = +\infty$, a continuous phase transition emerges from the quasibrittle to the brittle phase, and we determined the critical exponents of the transition. Note that the modified gamma form of Eq. (12) of the burst size distribution has also been proposed for earthquake magnitude distributions to maintain a finite strain release rate in natural earthquake populations [43,44].

To characterize the statistics of breaking bursts at finite cutoff strength $\varepsilon_{\max}$, we determined the burst size distribution $p(\Delta)$ for several parameter sets along two straight lines inside the quasibrittle phase of the bundle (see Fig. 2). Figure 6 presents $p(\Delta)$ varying the disorder exponent μ at a constant finite upper cutoff $\varepsilon_{\max}$. It can be seen that approaching the phase boundary $\mu \rightarrow \mu_c(\varepsilon_{\max})$ the burst size distribution tends to a power-law functional form followed by an exponential cutoff consistent with the generic expression (12). The value of the power-law exponent is the same $\tau = 3/2$ as for an infinite cutoff. As μ decreases from its critical value, the burst size distribution exhibits a crossover between two power-law regimes, i.e., the power law of exponent $\tau = 3/2$ is followed by a steeper one of exponent $\tau = 5/2$ in the regime of large bursts. For decreasing μ the crossover burst size Δ_0 separating the two power-law regimes, shifts to lower values. In the limit $\mu \rightarrow 0$ almost the complete size distribution can be described by a single power law of exponent $5/2$; however, the crossover burst size takes a small but finite minimum value.
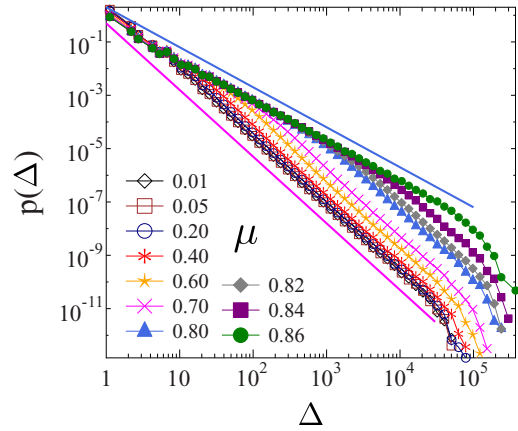

FIG. 6. Burst size distributions $p(\Delta)$ in a bundle of size $N = 10^7$ at a fixed upper cutoff $\varepsilon_{\max} = 10$ varying the value of the exponent μ. The two straight lines represent power laws of exponent $3/2$ and $5/2$.

For moderate amount of disorder, it has been shown for fiber bundles under equal load-sharing conditions that the size distribution of avalanches has a power-law functional form with a universal exponent $\tau = 5/2$ [29]. The result proved to be valid for those threshold distributions extending down to zero strength and having a sufficiently fast decreasing tail, where the constitutive curve $\sigma(\varepsilon)$ has a quadratic maximum [29,41]. In our system, the reason for the crossover of the burst size distribution $p(\Delta)$ between two power laws of exponent $3/2$ and $5/2$ is that the lower bound of fibers' strength $\varepsilon_{\min}$ has a finite nonzero value. Additionally, close to the boundary of the quasibrittle phase, bursts are generated in a narrow strain interval since the breakdown point ε_c falls close to $\varepsilon_{\min}$. It was pointed out in Refs. [14,45] that in such cases the crossover burst size Δ_0 can be obtained as

$$\Delta_0 = \frac{2}{a'(\varepsilon_c)(\varepsilon_c - \varepsilon_{\min})^2}, \qquad (15)$$

where $a'(\varepsilon_c)$ denotes the derivative of $a(\varepsilon)$ at the breakdown point. To apply this generic result to our truncated fat-tailed disorder distribution, we substitute Eqs. (4) and (9), which yields

$$\Delta_0 = \frac{2\varepsilon_{\max}(1 - \mu)^{1/\mu - 1}}{[\varepsilon_{\max}(1 - \mu)^{1/\mu} - \varepsilon_{\min}]^2}. \qquad (16)$$

This expression is valid for exponents $0 < \mu \leqslant \mu_c(\varepsilon_{\max})$. It can be seen in Eq. (16) that approaching the phase boundary $\mu \rightarrow \mu_c(\varepsilon_{\max})$, the crossover size diverges $\Delta_0 \rightarrow +\infty$, and hence, the burst size distribution $p(\Delta)$ has a single power-law regime of exponent $\tau = 3/2$. The crossover to a higher exponent $\tau = 5/2$ for large bursts is observed away from the phase boundary where Δ_0 takes finite values (see Fig. 6). Starting from Eq. (16), it can simply be shown that the divergence is described by a power law

$$\Delta_0 \sim (\mu_c - \mu)^{-\gamma}, \qquad (17)$$

with a universal exponent $\gamma = 2$. To test the validity of this prediction Eq. (17), we determined the value of Δ_0 numerically as the crossing point of fitted power laws of exponents
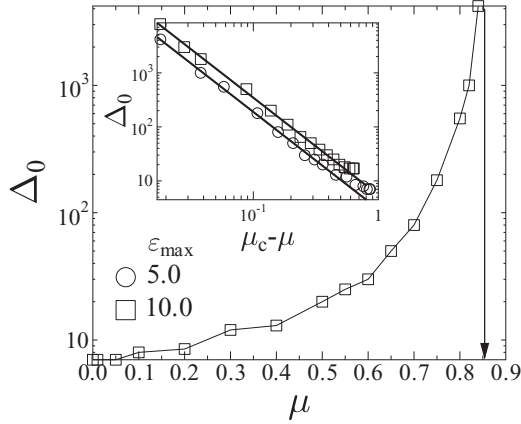
FIG. 7. Crossover burst size Δ_0 as a function of the disorder exponent μ for the cutoff strength $\varepsilon_{\max} = 10$. The arrow indicates the position of the corresponding critical point μ_c. The inset presents Δ_0 as a function of the distance from the critical point $\mu_c(\varepsilon_{\max}) - \mu$ for two upper cutoffs on a double logarithmic plot.

3/2 and 5/2. Figure 7 demonstrates that the crossover burst size Δ_0 rapidly increases as μ_c is approached, and it has a power-law dependence on the distance from the critical point $\mu_c - \mu$, in agreement with Eq. (17). The exponent of the fitted power law is $\gamma = 1.87 \pm 0.1$, which falls close to the analytical prediction.

IV. SIZE-DEPENDENT AVALANCHE STATISTICS

When the cutoff strength $\varepsilon_{\max}$ is varied while keeping the disorder exponent μ fixed, the burst size distribution exhibits an even more complicated behavior. For a fixed μ, we express the cutoff strength relative to the phase boundary using the parameter $\lambda = \varepsilon_{\max}/\varepsilon_{\max}^c$, which takes values in the range $\lambda > 1$. Figure 8 presents $p(\Delta)$ for several values of λ at the disorder exponent $\mu = 0.85$, i.e., along the vertical dashed line inside the quasibrittle phase of Fig. 2. It can be observed that starting from a single power law of exponent $\tau = 3/2$ at
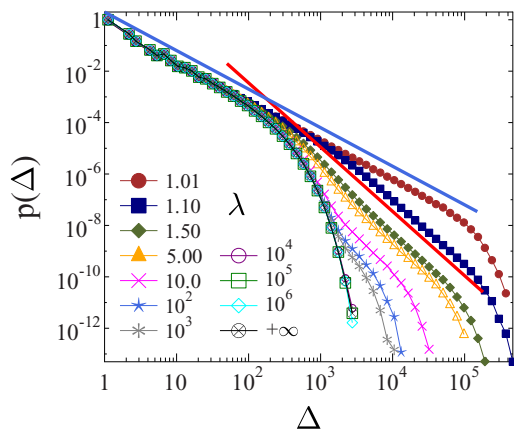

FIG. 8. Burst size distributions $p(\Delta)$ for a fixed value of the exponent $\mu = 0.85$ varying the upper cutoff λ. The bundle is composed of 10^7 fibers. The two straight lines represent power laws of exponent 3/2 and 5/2. The case of an infinite upper cutoff $\lambda = +\infty$ is also included for comparison.
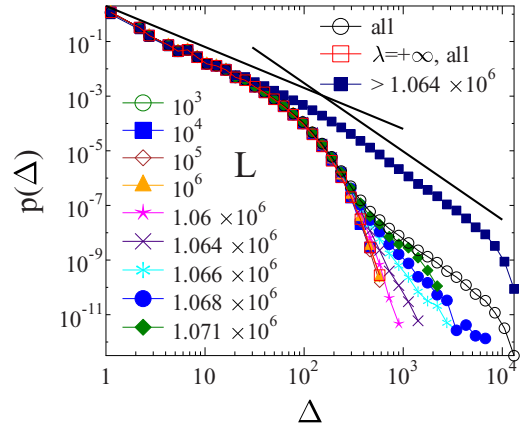

FIG. 9. Size distributions $p(\Delta)$ of the first L bursts of a bundle of $N = 10^7$ fibers varying L in a broad range at the fixed disorder parameters $\mu = 0.8$ and $\lambda = 500$. The complete distribution of the entire failure process is also presented together with the distribution of the last events just preceding global failure. The total number of events is about 1.08×10^6. The two straight lines represent power laws of exponents 3/2 and 5/2.

the phase boundary, $p(\Delta)$ shows again a crossover between two power-law regimes, where the crossover burst size Δ_0 shifts to lower values as λ increases. Starting from Eq. (16) it is easy to show that Δ_0 exhibits again a power-law divergence

$$\Delta_0 \sim (\lambda - 1)^{-\gamma}, \qquad (18)$$

when approaching the phase boundary $\lambda \to 1$. The value of the exponent γ is the same $\gamma = 2$ as in Eq. (17). However, a significant difference, compared to the case of a constant cutoff, is that far from the phase boundary, after some transients, the steeper power-law regime of exponent $\tau = 5/2$ gradually disappears. A single power law remains with exponent $\tau = 3/2$, as at the phase boundary Eq. (12), but with a significantly lower cutoff burst size Δ^*.

It is important to note in Fig. 8 that at sufficiently large cutoffs $\lambda > 1000$, the burst size distributions coincide with the one corresponding to the infinite cutoff $\lambda = +\infty$, in spite of the fact that the system has a finite critical point ε_c. The reason is that, at the μ exponent considered, the beginning of the series of bursts is close to stationary as has been illustrated in Fig. 3(a). Since the average number of triggered breakings $a(\varepsilon)$ is nearly constant over a broad range of strain ε, as λ increases, the critical point is preceded by a shorter and shorter accelerating regime, which has a diminishing contribution to the entire distribution $p(\Delta)$.

To test this idea we analyzed in detail the statistics of burst sizes in a bundle of size $N = 10^7$ at the disorder parameters $\mu = 0.8$ and $\lambda = 500$ where both power-law regimes are present. Figure 9 shows the burst size distribution $p(\Delta, L)$ evaluated in event windows containing the first L bursts, i.e., $p(\Delta, L)$ is the size distribution of bursts Δ_i, $i = 1, \ldots, L$, averaged over several realizations of the disorder at a given value of L. For comparison, the size distribution of the entire failure process is also presented together with the one corresponding to the case of an infinite cutoff $\lambda = +\infty$ obtained at the same system size N and μ exponent. It can be seen that up to the first $L \approx 10^6$ bursts, the distributions $p(\Delta, L)$ perfectly agree with
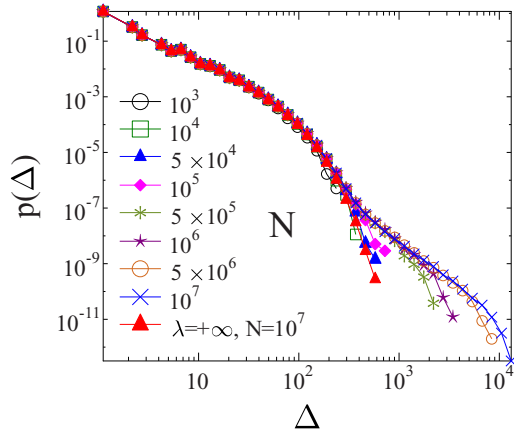
FIG. 10. Size distribution of bursts $p(\Delta)$ for different system sizes N at fixed values of the disorder parameters $\mu = 0.8$ and $\lambda = 500$. For small system sizes $p(\Delta)$ agrees with the corresponding distribution of the infinite cutoff $\lambda = +\infty$. Above a characteristic system size a second power-law regime gradually develops for large bursts.
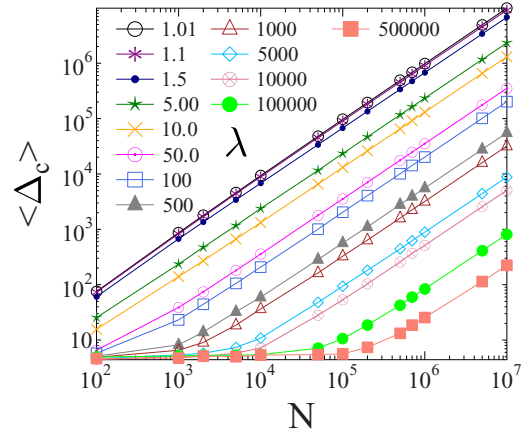

FIG. 11. Average size of the catastrophic avalanche $\langle \Delta_c \rangle$ as a function of the system size N for several values of the upper cutoff λ of fibers strength at a fixed exponent $\mu = 0.8$.

the case of an infinite cutoff $p(\Delta, \lambda = +\infty)$. Deviations from $p(\Delta, \lambda = +\infty)$ start around $L \approx 1.06 \times 10^6$ above which gradually a steeper power-law regime develops. The result confirms that in spite of the existence of a well-defined critical point ε_c, for a broad event range the statistics of burst sizes is consistent with the stationary process of the infinite strength cutoff, and acceleration towards failure is restricted to the close vicinity of ε_c. The argument is further supported by the size distribution of the last bursts with event index greater than $L = 1.064 \times 10^6$, which are generated in the vicinity of global failure. In this regime the functional form of $p(\Delta)$ is consistent with what has been obtained for varying μ in Fig. 6, i.e., a crossover emerges between two power laws of exponents $\tau = 3/2$ and $\tau = 5/2$, as expected in the vicinity of the critical point.

In Ref. [38] we have shown that for fat-tailed distributions of fiber strength, the number of fibers N has a substantial effect on the ultimate failure strength of the bundle: for small system sizes the strongest fiber controls the macroscopic failure, and consequently the average bundle strength increases with the system size N described by Eq. (7). The number of fibers N has to exceed a characteristic value to observe the usual decreasing trend towards the strength of the infinite system given by Eqs. (4) and (5). Since at large λ the system size N controls the behavior of the system at the critical point, it follows that N must play a decisive role also for the statistics of breaking avalanches. This is illustrated in Fig. 10, which presents burst size distributions of bundles of different sizes N at fixed values of the disorder parameters $\mu = 0.8$ and $\lambda = 500$. It can be observed that for small N values, the burst size distributions $p(\Delta)$ coincide with the corresponding curve of a large system $N = 10^7$ obtained at the infinite cutoff $\lambda = +\infty$. Above the system size $N \approx 10^5$ a second power-law regime gradually develops as has been observed in Fig. 9 for a single system size $N = 10^7$ with varying event window L.

The reason of this astonishing dependence of the statistics of avalanches on the size of the system is that for small

system sizes, even for finite cutoff strength of fibers, global failure occurs when the strongest fiber breaks. Consequently, the entire sequence of bursts is close to stationary, and their statistics is practically the same as for the infinite cutoff. The existence of a finite critical point ε_c is realized only when the system size N exceeds a characteristic value N_c. For bundles with $N > N_c$ global failure is preceded by an acceleration of the failure process with increasing burst sizes. In this regime macroscopic failure occurs in the form of a catastrophic avalanche; however, the catastrophic event is completely absent for $N < N_c$. In order to quantify this crossover of the avalanche statistics with respect to the size of the system N, we determined the average size of the catastrophic avalanche $\langle \Delta_c \rangle$ as a function of the size of the bundle N varying the upper cutoff of fibers' strength λ in a broad range. The size of the catastrophic avalanche can be estimated as

$$\langle \Delta_c \rangle \sim N[1 - P(\varepsilon_c)], \tag{19}$$

so that if a well-defined critical bundle strength ε_c exists, a linear dependence is obtained on the system size $\langle \Delta_c \rangle \sim N$. Figure 11 shows that for low λ values the simulation results are consistent with the above prediction. However, far from the phase boundary $\lambda > 1000$, a more complex behavior is obtained: for small system sizes $\langle \Delta_c \rangle$ does not depend on N, it takes a small constant value $\langle \Delta_c \rangle \approx 7$. The regular linear increase with N is restored above a characteristic system size N_c, which increases with λ. Figure 12 demonstrates that rescaling N with the μth power of λ, the curves of $\langle \Delta_c \rangle$ obtained at different λ values can be collapsed on the top of each other. The high-quality data collapse implies that the characteristic system size N_c, separating the two types of avalanche statistics, has a power-law dependence on λ as

$$N_c \sim \lambda^{\mu}. \tag{20}$$

This characteristic value N_c is of course the same as the one which controls the size scaling of the ultimate strength of the bundle (8) [38]. It also follows that the event window analysis presented in Fig. 9 can be performed only for system sizes $N > N_c$, and the crossover event index L_c below which the
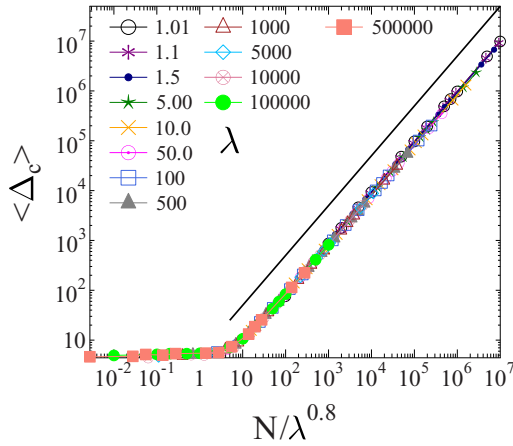
FIG. 12. The same data as in Fig. 11 are presented in such a way that along the horizontal axis the system size N is rescaled with λ^μ. High-quality data collapse is obtained. The straight line represents a power law of exponent 1.

burst size distribution is close to the one of the infinite cutoff has the same dependence (20) on the disorder parameter.

V. DISCUSSION

The degree of materials disorder has a substantial effect on the fracture of heterogeneous materials on both the micro- and macroscales. When subject to a slowly increasing external load, fracture proceeds in bursts which can be considered as precursors of global failure. Failure forecast methods of the imminent catastrophic failure strongly rely on the bursting dynamics [11,46,47]. It has been demonstrated experimentally that increasing amount of disorder gives rise to a more inten- sive precursory activity, which then improves the quality of forecasts [11,12].

In this paper we investigated the effect of the amount of disorder on the microscopic dynamics of the fracture process of heterogeneous materials in the framework of a FBM fo- cusing on the limit of very high disorder. We considered a power-law distribution of fibers' strength where the degree of disorder could be controlled by tuning the power-law expo- nent and the upper cutoff of breaking thresholds. Assuming equal load sharing after local breakings, we showed that on the macroscale the mechanical response of the bundle is either perfectly brittle where the bundle abruptly fails right at the breaking of the first fiber, or it is quasibrittle where macroscopic failure is approached through a sequence of breaking bursts.The evolution of the crackling event series and the statistics of burst sizes have a high importance for the forecasting of the imminent failure of the bundle.

We showed that for an infinite upper cutoff of fibers' strength, the sequence of bursts is stationary in the sense that the average burst size is constant. Hence, the system does not exhibit any sign of acceleration towards failure. Consequently, a power-law burst size distribution is obtained, where the disorder exponent only controls the cutoff burst size. For finite upper cutoffs we showed that there exists a well-defined critical point of global failure; however, it can be realized

only in sufficiently large systems. In small systems the global strength of the bundle is controlled by the strongest fiber. This peculiar behavior gives rise to an astonishing dependence of the statistics of burst sizes on the size of the system: for small systems the burst sequence proved to be close to stationary, and hence, the burst size distribution coincides with the one corresponding to the infinite upper cutoff of fibers' strength. For large systems the initially stationary sequence is followed by an accelerating regime in the close vicinity of the critical point, which gives rise to a crossover between two power laws of the burst size distribution. Analyzing the dependence of the average size of the catastrophic burst on the size of the bundle, we pointed out that the transition between the two types of burst size distributions occurs at a characteristic system size which depends on the disorder parameters of the bundle. The results can have relevance for the design of laboratory experiments: when the microscale materials disorder has a rapidly (exponentially) decaying distribution, the sample size mainly affects the cutoff of the size distribution of bursts but not its functional form. However, for fat-tailed disorder the sample size has a strong effect on the functional form of the burst size distribution so that the size of specimens in laboratory tests has to be sufficiently large to reproduce the acceleration of the burst sequence towards failure obtained in field measurements.

We also demonstrated that for a moderate amount of disor- der, i.e., varying the disorder parameters in the vicinity of the phase boundary between the brittle and quasibrittle phases, a crossover occurs between two power laws of exponents 3/2 and 5/2. The reason is that bursts are generated in a narrow strain interval close to the critical point of macroscopic failure. In this case the crossover burst size was found to have a power-law divergence as the phase boundary is approached.

Our results set important limitations on the forecastability of the imminent failure [11,17,18] of the system when the mi- croscale disorder is fat tailed. We have demonstrated that even if a considerable avalanche activity accompanies the failure process, the collapse may not be predictable either because it is controlled by the extreme order statistics of fibers' strength, or the accelerating regime preceding failure is too short. In failure forecast methods accelerating precursors have to be identified above a null hypothesis of stationary event rate, then one needs to wait for a sufficient amount of data to define a singularity with accuracy and precision at a finite time before the time of ultimate failure [18]. The effect of high disorder on the statistics of breaking bursts, revealed by our study, may be a real limitation for practical applications of forecasting methods based on acoustic or seismic precursors of failure [18,48].

In the present study we focused mainly on the integrated statistics of burst sizes considering all events up to failure. The quantitative characterization of the evolution of the event series towards failure requires further careful analysis, which is in progress.

[1] A. Petri, G. Paparo, A. Vespignani, A. Alippi, and M. Costantini, Phys. Rev. Lett. **73**, 3423 (1994).

[2] C. Maes, A. V. Moffaert, H. Frederix, and H. Strauven, Phys. Rev. B **57**, 4987 (1998).

[3] S. Deschanel, L. Vanel, N. Godin, and S. Ciliberto, J. Stat. Mech.: Theor. Exp. (2009) P01018.

[4] P. O. Castillo-Villa, J. Baró, A. Planes, E. K. H. Salje, P. Sellappan, W. M. Kriven, and E. Vives, J. Phys.: Cond. Matt. **25**, 292202 (2013).

[5] T. Mäkinen, A. Miksic, M. Ovaska, and M. J. Alava, Phys. Rev. Lett. **115**, 055501 (2015).

[6] J. Baró, P. Shyu, S. Pang, I. M. Jasiuk, E. Vives, E. K. H. Salje, and A. Planes, Phys. Rev. E **93**, 053001 (2016).

[7] P. Diodati, F. Marchesoni, and S. Piazza, Phys. Rev. Lett. **67**, 2239 (1991).

[8] D. Lockner, Intl J. Rock Mech. Mining Sci. Geomech. Abs. **30**, 883 (1993).

[9] M. B. J. Meinders and T. v. Vliet, Phys. Rev. E **77**, 036116 (2008).

[10] G. Niccolini, A. Carpinteri, G. Lacidogna, and A. Manuello, Phys. Rev. Lett. **106**, 108503 (2011).

[11] J. Vasseur, F. B. Wadsworth, Y. Lavallée, A. F. Bell, I. G. Main, and D. B. Dingwell, Sci. Rep. **5**, 13259 (2015).

[12] X. Jiang, H. Liu, I. G. Main, and E. K. H. Salje, Phys. Rev. E **96**, 023004 (2017).

[13] J. Koivisto, M. Ovaska, A. Miksic, L. Laurson, and M. J. Alava, Phys. Rev. E **94**, 023002 (2016).

[14] S. Pradhan, A. Hansen, and P. C. Hemmer, Phys. Rev. Lett. **95**, 125501 (2005).

[15] J. Davidsen, S. Stanchits, and G. Dresen, Phys. Rev. Lett. **98**, 125502 (2007).

[16] D. Sornette, Proc. Natl. Acad. Sci. U. S. A. **99**, 2522 (2002).

[17] B. Voight, Nature (London) **332**, 125 (1988).

[18] A. F. Bell, M. Naylor, and I. G. Main, Geophys. J. Int. **194**, 1541 (2013).

[19] J. Rosti, X. Illa, J. Koivisto, and M. J. Alava, J. Phys. D **42**, 214013 (2009).

[20] Y. Xu, A. G. Borrego, A. Planes, X. Ding, and E. Vives, Phys. Rev. E **99**, 033001 (2019).

[21] S. Zapperi, P. Ray, H. E. Stanley, and A. Vespignani, Phys. Rev. Lett. **78**, 1408 (1997).

[22] C. B. Picallo, J. M. López, S. Zapperi, and M. J. Alava, Phys. Rev. Lett. **105**, 155502 (2010).

[23] A. Guarino, A. Garcimartin, and S. Ciliberto, Eur. Phys. J. B **6**, 13 (1998).

[24] O. Ramos, P.-P. Cortet, S. Ciliberto, and L. Vanel, Phys. Rev. Lett. **110**, 165506 (2013).

[25] S. Santucci, L. Vanel, and S. Ciliberto, Phys. Rev. Lett. **93**, 095505 (2004).

[26] L. de Arcangelis, A. Hansen, H. J. Herrmann, and S. Roux, Phys. Rev. B **40**, 877 (1989).

[27] J. V. Andersen, D. Sornette, and K.-t. Leung, Phys. Rev. Lett. **78**, 2140 (1997).

[28] A. Hansen, P. Hemmer, and S. Pradhan, *The Fiber Bundle Model: Modeling Failure in Materials*, Statistical Physics of Fracture and Breakdown Vol. 2 (Wiley, Berlin, 2015).

[29] M. Kloster, A. Hansen, and P. C. Hemmer, Phys. Rev. E **56**, 2615 (1997).

[30] F. Kun, F. Raischel, R. C. Hidalgo, and H. J. Herrmann, in *Modelling Critical and Catastrophic Phenomena in Geoscience: A Statistical Physics Approach*, Lecture Notes in Physics Vol. 705, edited by P. Bhattacharyya and B. K. Chakrabarti (Springer-Verlag, Berlin, 2006), pp. 57–92.

[31] R. C. Hidalgo, K. Kovács, I. Pagonabarraga, and F. Kun, Europhys. Lett. **81**, 54005 (2008).

[32] R. C. Hidalgo, F. Kun, K. Kovács, and I. Pagonabarraga, Phys. Rev. E **80**, 051108 (2009).

[33] S. Roy, S. Biswas, and P. Ray, Phys. Rev. E **96**, 063003 (2017).

[34] S. Roy and P. Ray, Europhys. Lett. **112**, 26004 (2015).

[35] K. Kovács, R. C. Hidalgo, I. Pagonabarraga, and F. Kun, Phys. Rev. E **87**, 042816 (2013).

[36] E. Karpas and F. Kun, Europhys. Lett. **95**, 16004 (2011).

[37] S. Hao, H. Yang, and X. Liang, Materials **10**, 515 (2017).

[38] V. Kádár, Z. Danku, and F. Kun, Phys. Rev. E **96**, 033001 (2017).

[39] R. L. Smith, Proc. R. Soc. London A **372**, 539 (1980).

[40] R. L. Smith, S. L. Phoenix, M. R. Greenfield, R. B. Henstenburg, and R. E. Pitt, Proc. R. Soc. London A **388**, 353 (1983).

[41] P. C. Hemmer and A. Hansen, J. Appl. Mech. **59**, 909 (1992).

[42] Z. Danku and F. Kun, J. Stat. Mech.: Theor. Exp. (2016) 073211.

[43] I. G. Main and P. W. Burton, Bull. Seismol. Soc. Am. **74**, 1409 (1984).

[44] Y. Kagan, Geophys. J. Int. **106**, 123 (1991).

[45] S. Pradhan, A. Hansen, and P. C. Hemmer, Phys. Rev. E **74**, 016122 (2006).

[46] B. Voight, Science **243**, 200 (1989).

[47] M. Tárraga, R. Carniel, R. Ortiz, and A. García, in *Caldera Volcanism: Analysis, Modelling and Response*, Developments in Volcanology, Vol. 10, edited by J. Gottsmann and J. Marti (Elsevier, Amsterdam, 2008), pp. 447–469.

[48] R. J. Geller, D. D. Jackson, Y. Y. Kagan, and F. Mulargia, Science **275**, 1616 (1997).